Journal of Catalysis 265 (2009) iii–vi

Contents lists available at ScienceDirect

Journal of Catalysis

journal homepage: www.elsevier.com/locate/jcat

Journal of Catalysis Vol. 265, Issue 1, 2009

Contents

REGULAR ARTICLES

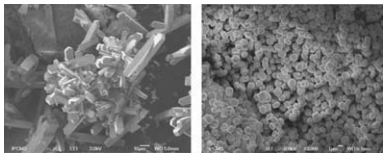

The influence of the zeolite ZSM-5 synthesis procedure (hydroxide and fluoride route) on its catalytic performances in the Methanol to Olefin (MTO) reaction has been investigated. In addition, a new concept in the preparation of zeolite materials has been employed, so-called in-situ zeolite synthesis. The silica superficial layer from the support itself was used as a silica source in this procedure. Depending on the preparation procedure, structured zeolite catalysts exhibited different performances in terms of activity and selectivity.

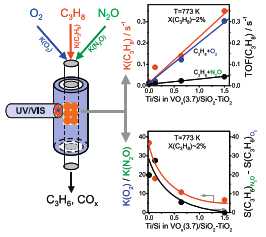

Time-resolved in situ UV/Vis spectroscopy related the activity and selectivity of highly dispersed VO_x species over Ti–Si-MCM-41 materials in propane oxidation to propene with the constants of reduction ($K(C_3H_8)$) and reoxidation ($K(O_2)$, $K(N_2O)$) of these species.

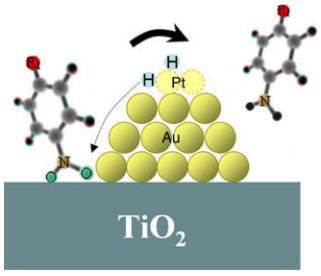

Bimetallic gold–platinum catalysts with optimised Pt contents have been designed through kinetic and isotopic studies, showing the highest activity reported up to now for the chemoselective hydrogenation of substituted nitroaromatic compounds.

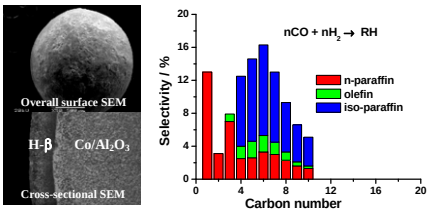

A H–β zeolite coating has been directly applied over Co/Al_2O_3 pellets by a hydrothermal synthesis method. This tailor-made encapsulated catalyst possesses extremely high spatial selectivity for isoparaffin synthesis from syngas.

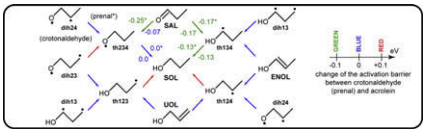

From an original use of generalized Brönsted–Evans–Polanyi relations and density functional theory calculations, the key question of the selectivity of the hydrogenation of unsaturated aldehydes on Pt(1 1 1) has been elucidated. In particular, the enhanced selectivity to SOL (saturated alcohol) is explained by a significant lowering of the surface transformation barriers from SAL (saturated aldehyde) to SOL.

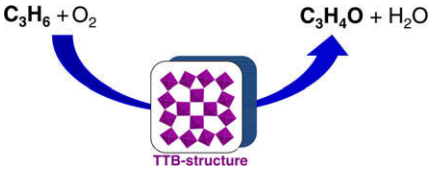

Te-containing multicomponent Mo-based catalysts presenting tetragonal tungsten bronze (TTB) structure show high selectivity in the partial oxidation of propene to acrolein. The highest yield to acrolein achieved with Te/Mo atomic ratios in bulk of 0.03.

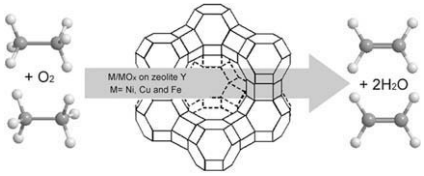

Metal-loaded zeolite Y catalyzed oxidative dehydrogenation of C_2H_6 to C_2H_4.

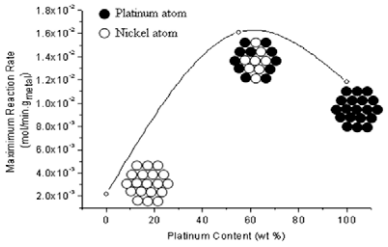

Pt/Ni–silica catalysts were prepared via co and step impregnation using $NaBH_4$ as a reducing agent. $Pt_{55}Ni_{45}$-CI (co-impregnated) exhibited superior reactivity compared to the monometallic catalysts. Alloying and Pt segregation may contribute to this enhanced activity.

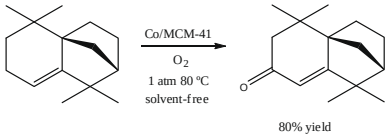

Co-MCM-41, which contains cobalt incorporated into the framework, is an efficient, environmentally friendly solid catalyst for the liquid-phase aerobic oxidation of isolongifolene into isolongifolen-9-one which is highly valuable for perfume industry.

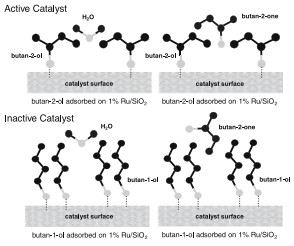

Deactivation of a Ru/SiO_2 catalyst for butan-2-one hydrogenation in water has been found to be associated with the formation of $Ru(OH)_x$; however, this effect may be mitigated by the presence of secondary alcohols which form a hydrophobic surface coating.

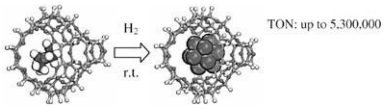

Pd clusters generated in the supercage of a USY zeolite worked as efficient catalysts in the Suzuki–Miyaura reactions.

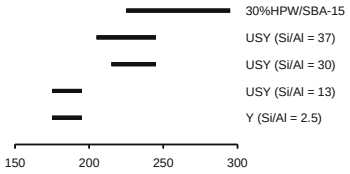

Temperature where *n*-decane hydroisomerization yield exceeds 45%.

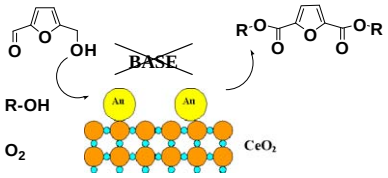

Gold nanoparticles supported onto nanoparticulated cerium oxide catalyzed the oxidative esterification of HMF into DMF with oxygen and *n*-alcohols in the absence of a base.

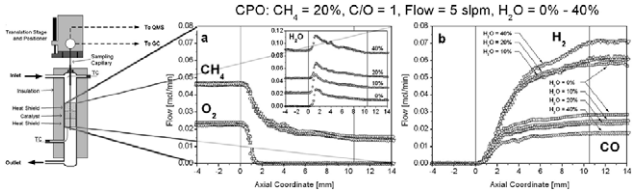

Spatial profiles of autothermal methane CPO on Rh-based catalysts illustrate the effects of H_2O and CO_2 addition on mass transfer, water gas shift, and steam reforming.